Interaction behavior of sand-diluted and mixed Fe-based oxygen carriers with potassium salts

Fuel 339 (2023) 127372

Contents lists available at ScienceDirect

Fuel

journal homepage: www.elsevier.com/locate/fuel

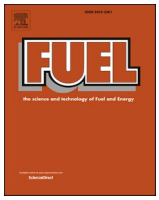

Interaction behavior of sand-diluted and mixed Fe-based oxygen carriers with potassium salts

Fredrik Hildor [a,*], Duygu Yilmaz [a,b], Henrik Leion [a]

[a] Energy and Materials, Chemistry and Chemical Engineering, Chalmers University of Technology, 412 96 Gothenburg, Sweden
[b] Institute for Energy Technology (IFE), Department of Environmental Industrial Processes, Instituttveien 18, 2007 Kjeller, Norway

ARTICLE INFO

Keywords:
Oxygen carrier
Ilmenite
LD slag
Agglomeration
Alkali

ABSTRACT

Oxygen carriers, in the form of metal oxide particles, are bed materials that transport oxygen in solid form in fluidized bed applications, such as in chemical-looping applications. In biofuel applications, it is well known that alkali from the fuel ash can react with the bed material and cause, among other operation issues, agglomeration. When using oxygen carriers in a fluidized bed, it is likely that the bed material is either a mixture of different metal oxide materials or partly diluted with sand. This is to improve or combine the chemical properties of the materials used or simply for economic reasons.

This work investigates how three potassium salts K_2CO_3, K_2SO_4 and KH_2PO_4 interact with the oxygen carriers: Steel converter slag (LD slag), ilmenite, mixtures of the two and each carrier diluted with silica sand. The salts were used as model compounds that can occur in biofuel ash. The set-up used was a fixed bed where a small sample of bed material is mixed with a potassium salt equivalent to 4 wt-% of potassium. The mixture was then exposed to reducing (H_2 in steam) conditions at 900 °C during several hours in a tubular furnace. This provides a worst-case scenario for solid–solid interaction in a fluidized bed. If a solid–solid reaction does not take place in this setup, it will most likely never occur in a fluidized bed.

When LD slag and ilmenite were combined, the potassium from the salts would prefer to accumulate in the ilmenite rather than the LD slag. Ca from LD slag interacted with KH_2PO_4 resulting in a less severe agglomeration than when ilmenite was used separately with the same salt. When the oxygen carriers were diluted with silica sand, potassium salt interaction resulted in agglomeration for both the oxygen carriers with all potassium salts. K_2CO_3 and K_2SO_4 formed potassium silicates, while KH_2PO_4 formed a phosphorus-containing melt. When LD slag was present, phosphorus was located in a K-Ca-P phase that was not present if ilmenite was present.

1. Introduction

Chemical Looping Combustion (CLC) and related processes that facilitate Carbon Capture and Storage (CCS) play an important role in society's efforts to pursue a sustainable future [1]. One way to deal with high levels of carbon dioxide in the atmosphere is to create negative emissions where the carbon dioxide from biomass combustion is captured and stored in the bedrock [2]. This can be achieved by combining the Chemical Looping Combustion (CLC) and Bioenergy with Carbon Capture and Storage (BECCS) processes [3,4]. Instead of air, oxygen carriers supply oxygen to the combustion process in CLC [5]. Therefore, nitrogen-free fuel gases can be collected, and carbon dioxide can be easily captured without energy consumption for the separation [6].

The CLC process consists of an air and a fuel reactor that can be both fluidized [7]. Oxygen carriers used in the CLC process can simply be shown as M_xO_y where M stands for a metal that can have different valance states, and O stands for oxygen. In the air reactor, a reduced oxygen carrier (M_xO_{y-1}) is oxidized by an oxidizing atmosphere, generally air. In the fuel reactor, this oxidized oxygen carrier (M_xO_y) is reduced to a metal oxide with a lower oxidation level (M_xO_{y-1}) by a reducing atmosphere[5]. Oxygen carriers can also be used as bed materials for conventional combustion in circulating fluidized bed (CFB) boilers, and this technology is referred to as Oxygen Carrier Aided Combustion (OCAC) [8]. The advantage of OCAC technology is the high technology readiness with over 12000 h operation at an industrially relevant scale [9]. OCAC is also relatively easy to implement by changing the bed material in already built conventional fluidized bed boilers and future

* Corresponding author.
E-mail address: fredrik.hildor@chalmers.se (F. Hildor).

https://doi.org/10.1016/j.fuel.2022.127372
Received 6 September 2022; Received in revised form 14 December 2022; Accepted 30 December 2022
Available online 6 January 2023

facilities designed in mind for CO_2 capture.

The reducing atmosphere can be a solid fuel, syngas or methane [10], and the selection of the oxygen carrier depends on the fuel attended for the process since oxygen carriers have different reactivity toward different fuels [11–13]. Even though fossil fuels are still the most used fuels to supply energy globally, biofuels are vital to sustain the supply and achieve negative emissions [14]. However, biomass-derived fuels generally contain a significant number of alkali-based compounds, along with other ash-forming matters which gives a highly reactive nature [15]. After the complete combustion of the fuel, there is an inorganic mixture remains that is called ash. The composition of the ash depends on the source of the fuel, and biomass generally contains Si, Al, Ti, Fe, Ca, Mg, Na, K, S, and P in its ash [16].

Oxygen carriers can be selected from metal oxide-based synthetic spinel structures, perovskites, minerals, and transitional metal oxide-bearing wastes [17–19]. Instead of a single type of metal oxide, sometimes a mixture of oxygen carriers or a mixture of oxygen carriers diluted with sand can be used to improve the chemical properties or to decrease the cost of the bed material [20]. Fe and Mn are among the most used transitional metals for oxygen carrier purposes due to their abundance, low-cost and high performance [21,22]. Especially Fe-based oxygen carriers can be generated from natural minerals such as ilmenite or from wastes such as steel slags. Ilmenite is an abundant natural mineral. Steel slags can be utilized in different applications to reduce waste, and its high Fe content [23] makes it also suitable for OCAC applications. Especially steel converter slag, also called LD (Linz-Donawitz) slag, which is a by-product of the basic oxygen steel production process, has been reported as a successful oxygen carrier [22,24].

Alkali-based compounds are well known to interact with silica present in the bed material or in the fuel to form low-melting-point alkali silicates [25–27]. Therefore, a major challenge during the utilization of biomass-derived fuel is ash-related issues [16,28,29]. During operation, the formed ash may deposit on tube walls and superheaters and clog the operation lines and heat transfer areas [27]. On the superheaters, it may cause corrosion due to the corrosive compounds in the ash [21]. In a fluidized bed, the ash may cause agglomeration of the bed material or if oxygen carriers are used, the reaction with ash may cause deactivation of the oxygen carriers [30,31]. Agglomeration of beds can occur when compounds with low melting point stick the particles together leading to the collapse of the fluidized bed. Two different mechanisms are observed for agglomeration: i) ash reacts with the bed material forming a new compound with low melting temperature or ii) the ash is inert towards the bed material, but has by itself a low melting temperature [32].

As the oxygen carrier will be directly affected by the formed ash, the selection of the oxygen carrier for a specific fuel should be done carefully, considering the known interaction between them [33,34]. For example, it is known that pure Fe oxides have tendency to agglomerate with the interaction of potassium chloride and phosphates [25,35]. Several studies have reported the interaction between ilmenite or LD slag and some potassium salts in lab scale [36,37] and with biofuel ash in a semi-industrial scale [21,38,39]. However, there is no systematic study that shows the effect of potassium salts on the combination of ilmenite or LD slag or when the oxygen carriers are diluted with sand. From a process perspective, mixtures of oxygen carriers or dilution with sand could be interesting both for cost savings and process management. Cost savings since e.g. silica sand and LD slag are less expensive than ilmenite [40,41]. Process management for adjusting the oxygen transfer in a chemical looping process [42] or adding e.g. LD slag as a source of lime to the process for sulfur control and ash interaction [43].

Investigation of the effect of potassium salts on the sand combined oxygen carrier is not only important for economic reasons but also for understanding the interaction mechanism as LD slag and ilmenite have relatively poor ability to absorb alkali compared to sand [22,39,44]. Therefore, ilmenite, LD slag and sand were combined as oxygen carriers to study the effect of the most commonly observed potassium salts under reducing atmospheres.

2. Experimental procedure

Ilmenite (provided by Titania AB) and LD slag (provided by SSAB) were used as the main oxygen carriers in the study. K_2CO_3 (Sigma Aldrich^{TM}), KH_2PO_4 (Alfa Aeasar^{TM}) and K_2SO_4 (Merck^{TM}) were used as potassium-based salts. Oxygen carriers were sieved into a 100–300 μm size range prior to use. Salts were simply ground with the use of agate mortar and pestle. The chemical analysis of ilmenite and LD slag is given in Table 1. Elemental analysis was performed with X-ray fluorescence (XRF) using a Panalytical Axios equipped with holders for powders. 0.5–1 g samples were pulverized using marble mortar and pestle before being analyzed. The column with SUM indicates the estimated amount of all identified species in their stable oxide, MgO, Al_2O_3, SiO_2, CaO, TiO_2, V_2O_5, P_2O_5, MnO and Fe_2O_3. If the SUM does not add up to 100, it is an indication that the elements are not present in an oxidized form or contain elements that are not detected using XRF, e.g. such as carbonates, hydroxides or crystalline water.

To mimic the conditions in an air reactor, LD slag and ilmenite were first oxidized separately at 900° C for 24 h to achieve complete oxidation. After the oxidation, the oxygen carriers were sieved into a 125–250 μm particle size range. Each tested batch in the study is given in Table 2 with the abbreviations as a sample name.

For each sample, oxygen carriers, either single or mixture were used with or without a potassium salt resulting in a total weight of 5 g. Samples were simply mixed with a potassium salt, and the amount of K in the sample was set to 4 wt-% of the oxygen carrier. This value was chosen as remained K in a bed of ilmenite used in a large-scale fluidized bed boiler and was reported as a maximum 4 wt-% [21]. When the samples were prepared, they were placed in an alumina boat crucible and inserted into a horizontal tube furnace. Each sample was reduced at 900 °C for 3 h under a reducing atmosphere consisting of 50 ml/min of nitrogen bubbled through a water bath and cooled to obtain a flow with nitrogen and saturated with steam at 60 °C (partial pressure of ≈20 vol-% H_2O) and 50 ml/min of Ar diluted H_2 gas mixture (5 vol-% H_2). The heating and cooling rate was set to 400 °C/h. An illustration of the experimental setup can be seen in Fig. 1.

After the reduction experiments, the samples were characterized by X-ray diffraction (XRD) (Bruker D8, Cu Kα, 40 kV, 40 mA) in the range $2\theta = 15 - 75^{\circ}$ with a step size of 0.01. For morphological investigation and elemental mapping, scanning electron microscopy (SEM) − energy-dispersive X-ray spectroscopy (EDX) (FEI Quanta 200 FEG ESEM and Phenom^{TM} Pro-X) were used. The samples were embedded in an epoxy mold and polished to investigate the cross-section of the particles. In this way, it would be possible to reveal the phases that caused agglomeration and bridging between particles.

3. Results and discussion

3.1. Effect of potassium salts on ilmenite diluted sand

Since samples only containing ilmenite and salts have already been investigated in a previous study [37] where the method, samples and results were almost identical, the unique part of this study is studied in this section. The results of experiments with ilmenite and salts in this work were coherent with the previous study [37]. In summary, when ilmenite (IL) was mixed with K_2CO_3 and K_2SO_4 no agglomeration was observed while agglomeration was observed for KH_2PO_4. Potassium from K_2CO_3 and K_2SO_4 did migrate into the structure of ilmenite while KH_2PO_4 decomposed forming KPO_3 that was associated with the surface of the particles. This melt acted as a flux containing small amounts of Fe. The phase analysis of i) oxidized, ii) reduced ilmenite and iii) K_2CO_3 mixed reduced ilmenite was analyzed with XRD. i) In oxidized ilmenite, the main phase was pseudobrookite, Fe_2TiO_5 along with some Ti-substituted hematite-structured ilmenite, $Fe_{2-x}Ti_xO_3$. ii) After the reduction, ilmenite ($Fe_{2-x}Ti_xO_3$) was the most dominant phase. iii) When K_2CO_3 salt was mixed with ilmenite and reduced in the horizontal

Table 1
Elemental analysis using XRF of the initial materials after heat treatment given in wt-%. Impurities that are lower than 0.3 wt-% were not included. SUM indicates if the amount of the oxides of the quantified elements adds up to the sample weight.

	SUM	Mg	Al	Si	Ca	Ti	V	Mn	Fe
LD slag	84.8	1.9	0.6	4.6	29.3	0.6	1.8	2.2	14.7
Ilmenite	100.0	2.1	0.6	1.6	0.3	25.4	–	0.16	33.8

Table 2
Tested samples in the study and this composition are given in wt-%.

Sample	Material	Composition (wt-%)
IL	Ilmenite	100
ILLD	Ilmenite and LD slag	50/50
LD	LD slag	100
ILSA	Ilmenite and sand	50/50
LDSA	LD slag and sand	50/50

furnace, the main phases were $Fe_{2-x}Ti_xO_3$ (where $0,1 < x < 0,8$)along with rutile (TiO_2) and priderite-based compounds (K-Fe-Ti oxide) was observed. Even though a homogeneous distribution of potassium was observed along with the ilmenite particles, higher concentrations of potassium could be observed in impurities containing Al and Si, most likely forming potassium aluminum silicates. However, no neck formation or bridging between the particles was observed which was consistent with the previous studies [37].

When the ilmenite was diluted with sand and reduced in presence of K_2CO_3, only minor concentrations of potassium were detected in the Al-Si-rich regions and inside the ilmenite particles. The highest concentration of potassium was found associated with silicon and suggesting the formation of a melt of potassium silicate that also resulted in severe agglomeration. This melt can be seen in Fig. 2 between the ilmenite and sand particles. As can be observed in the figure, some particles are broken due to the force of extracting the particles from the crucible.

When ilmenite (IL) was reduced in the presence of K_2SO_4, the sample behaved similarly to the ilmenite sample reduced with K_2CO_3. Potassium preferred to locate in Al-Si-rich regions and potassium could be detected throughout the ilmenite particles. Sulfur from the sulfate formed gaseous compounds and could not be detected with SEM-EDS. This was also coherent with previous studies [37,45].

When ilmenite was diluted with sand (ILSA) and reduced with K_2SO_4, agglomeration of the sample was observed. In SEM-EDS (Fig. 3) a phase connecting the particles containing potassium and silica was observed, forming a melt that coated the particles (C in Fig. 3). Potassium most likely forms potassium silicates that have a low melting point and causes bridging between particles[32]. Sulfur could not be detected in the sample suggesting that volatile sulfur species such as H_2S and SO_2 were formed due to the presence of steam [37]. This forms at the same time reactive KOH [37] that could react with the sand particles forming

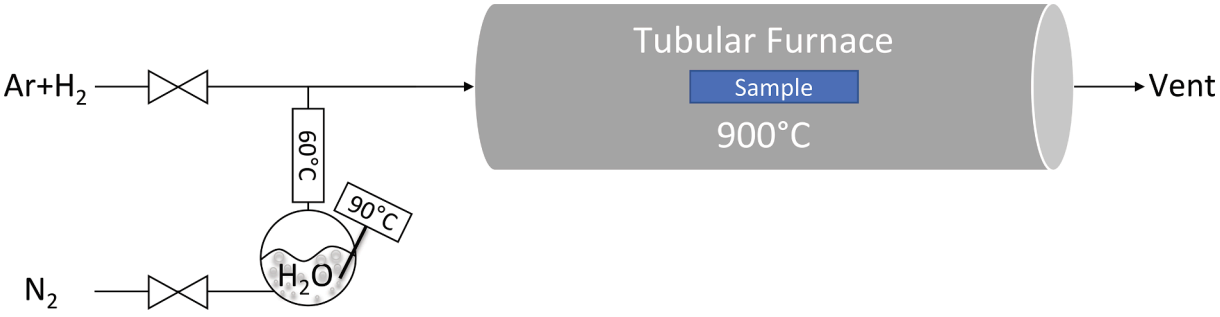

Fig. 1. Schematic layout of the horizontal tube furnace and the gas conditioner unit for saturated nitrogen with water.

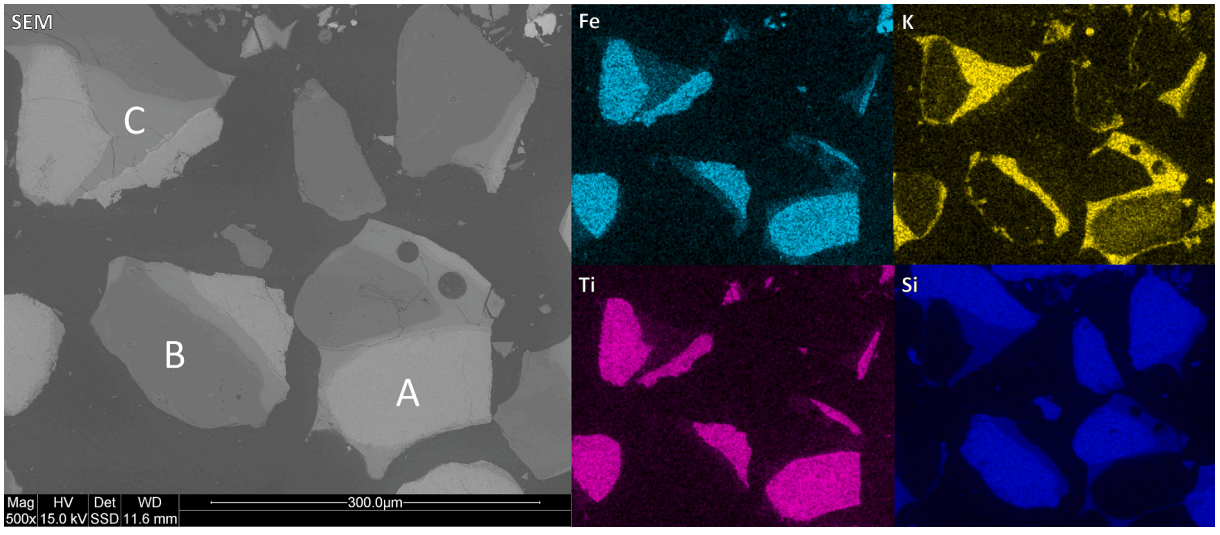

Fig. 2. Back-scattered SEM and elemental mapping micrographs of cross-sections of the reduced ilmenite/sand (ILSA)-K_2CO_3 mix sample. A: Ilmenite particle, B: Sand particle. C: Melt of potassium silicate.

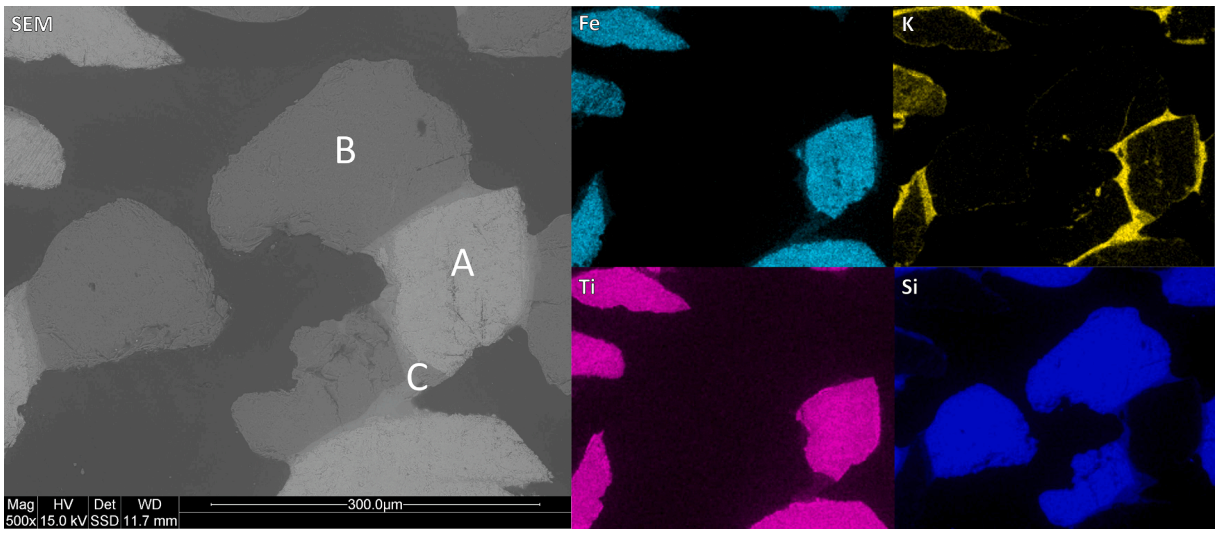

Fig. 3. Back-scattered SEM and elemental mapping micrographs of cross-sections of the reduced ilmenite/sand (ILSA)-K_2SO_4 mix sample. A: Ilmenite particle, B: Sand particle. C: Melt of potassium silicate.

potassium silicate.

Potassium and phosphorus containing salts are reported to have the harshest effect on Fe-oxides used as an oxygen carriers [25,36,46]. Consistent with the literature studies, potassium phosphate agglomerated the ilmenite particles without forming any silicate species. As KH_2PO_4 has a low melting point (252 °C), it decomposes into KPO_3 (melting point at 807 °C) via Reaction (1) [47,48]. When KPO_3 formed, it coated the ilmenite particles which caused an agglomeration. This observation was also reported in the literature [37]. When ilmenite was diluted with sand (Fig. 4), a similar case was observed. KPO_3 formed a melt coating the particles resulting in agglomeration. Iron was detected in the KPO_3 as iron had migrated into the flux, also seen in previous studies [37]. The silicon did not migrate nor react with the KPO_3, the KPO_3 only formed a layer on the particles.

$$KH_2PO_4 \rightarrow KPO_3 + H_2O \quad (1)$$

Among these three salts, the most significant agglomeration was observed when KH_2PO_4 was used as a salt with ilmenite oxygen carriers; and sand dilution did not change the behavior of the salt. The agglomeration observed for K_2CO_3 (Fig. 2) and K_2SO_4 (Fig. 3) was associated with the agglomeration mechanism where the alkali salt reacts with the sand particles forming potassium silicate. This is in contrast to the samples with KH_2PO_4 where the agglomeration was caused by the decomposition of the salt to KPO_3 which has a low melting temperature.

Both K_2CO_3 and K_2SO_4 are known to increase the reactivity of ilmenite toward carbon monoxide [37]. The reactivity are not monitored in this study, so the formation of potassium silicate on the surface of the particles has an unknown effect of the reactivity. In studies using coal ash containing silicon and minor amounts of alkali, no decrease in the reactivity of the iron-based oxygen carriers could be observed, even though most ashes were very well known to deactivate the bed material [49]. Therefore, it cannot be known for certain how the potassium silicate will affect the reactivity of the oxygen carrier.

3.2. *Effect of potassium salts on LD slag diluted with sand*

The phase analysis of LD slag via XRD showed that the main observed phase after the oxidation was Srebrodolskite ($Ca_2Fe_{2-x}Mn_xO_5$), Mn substituted Magnetite ($Fe_{3-x}Mn_xO_4$) along with Ca bearing phases such as Ca-silicates. After the reduction, srebrodolskite-based phases with different stoichiometric ratios were the main phases along with others. As the amount of salt was low in the system, no significant and reliable difference was observed related to alkali salt-based formation.

Since samples only containing LD slag and salts have already been investigated in a previous study [36] where the method, samples and results were almost identical to this work, only the results unique for this study are treated in this section.

Like ilmenite samples, potassium was located along with Si-rich

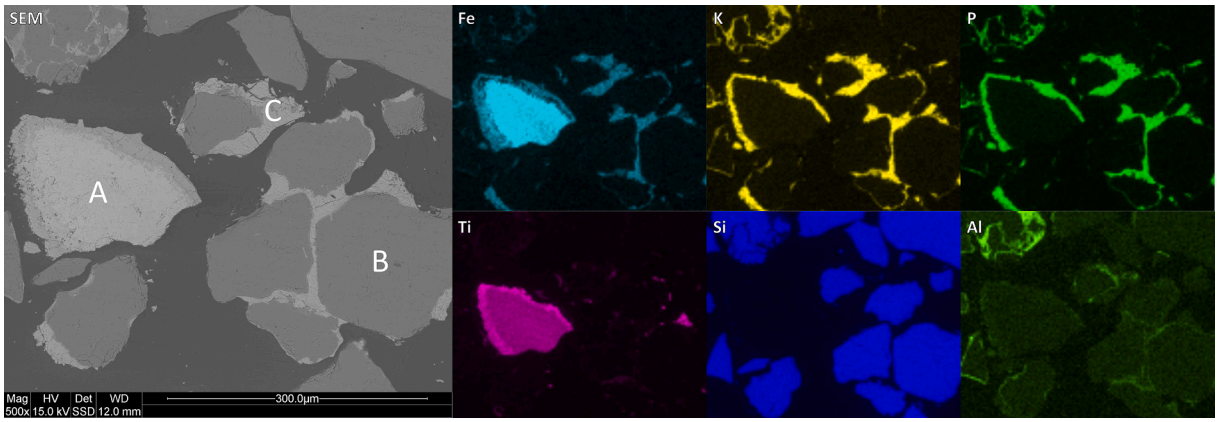

Fig. 4. Back-scattered SEM and elemental mapping micrographs of cross-sections of the reduced ilmenite/sand (ILSA)-KH_2PO_4 mix sample. A: Ilmenite particle, B: Sand particle. C: Melt containing potassium and phosphorus- KPO_3- with traces of Fe, Ti and Si.

regions when K_2CO_3 was used as salt with LD slag oxygen carriers diluted with sand. As with ilmenite, the salt and sand formed potassium silicate resulting in a severe agglomeration due to the melt between the particles (Fig. 5). However, this strong interaction between silica and K_2CO_3 may deactivate the oxygen carriers since LD slag may consist of several different Fe-bearing silicates [36,50].

When K_2SO_4 was used as a salt in the LDSA system, a significant agglomeration was observed which was most likely caused by low melting point potassium silicate formation (Fig. 6). Active oxygen carriers were surrounded by this alkali silicate formation which may reduce the gas permeability of the bed material and decrease the redox capacity of the oxygen carrier. The interaction of the potassium-bearing species with silica in the LD slag may take time; however, if there is unbound silica in the system, the formation of potassium silicate will be easier. As sand dilution would increase the amount of silica in the system, it may also increase the risk of agglomeration. Sulfur could only be detected together with calcium in the sample suggesting partial formation of $CaSO_4$.

Like the ilmenite system, KH_2PO_4 was the harshest salt among the tested potassium salts on the LD slag. However, compared to the IL and ILSA systems where potassium and phosphorus were located together as KPO_3 the phosphorus interacts will the calcium in the LD slag. Phosphorus was concentrated together with calcium and potassium around the LD slag. This has been observed for LD slag in previous studies and was observed to not affect reactivity towards carbon monoxide as significantly as KH_2PO_4 with ilmenite [36,37]. In the LDSA-KH_2PO_4 system displayed in Fig. 7, there was also potassium silicate formation observed free of phosphorus (C in Fig. 7). This indicates that the calcium in LD slag acts as lime addition to prevent agglomeration in boilers operated with high phosphorus fuel forming high melting temperature Ca-K-P phase (D in Fig. 7) [51,52]. However, these samples were agglomerated as the previous samples with melts either of potassium silicates or melts containing Ca-K-P.

3.3. Effect of potassium salts on ilmenite diluted with LD slag

The interaction of K_2CO_3 and mixed LD slag/ilmenite oxygen carriers was like the previous cases in this study. When the combination of these two different oxygen carriers was used, potassium was preferentially located in the ilmenite particles (Fig. 8). The same phenomena were also observed when K_2SO_4 was used as a salt (Fig. 9). Potassium was mainly associated with the ilmenite particles and Al-Si impurities. In the ilmenite particles potassium iron titanates were formed that were also detected in the XRD pattern of the related samples as in previous studies [37] as with samples with only ilmenite with either K_2CO_3 or K_2SO_4.

Sulfur originating from K_2SO_4 was only detected in minor amounts and mostly together with calcium in the LD slag particles, the same as observed in the LD slag diluted with silica sand sample. Besides this minor sulfur content, no major differences could be detected between the carbonate and sulfate salts.

KH_2PO_4 was the harshest salt on both ilmenite and LD slag-based oxygen carriers when these oxygen carriers were mixed with KH_2PO_4 individually. The same results were also observed for the mixed oxygen carrier test (Fig. 10). A significant agglomeration formed due to the formation of a K-Ca-P containing phase when the mixed oxygen carriers were combined with KH_2PO_4. Some potassium was observed to be integrated into the ilmenite particles, but the majority was in the Ca-K-P phase (C in Fig. 10). This potassium phosphate layer coated each individual particle regardless of the type of oxygen carrier. This formation behaved as a network to connect the ilmenite and LD slag particles via covering the outer layer of the oxygen carriers.

3.4. Overview of agglomeration and elemental composition

An overview of the agglomeration behavior of the tested samples can be observed in Table 3. Here it can be observed that, as in previous studies, phosphate-induced agglomeration to all tested materials [36,37]. With K_2CO_3 and K_2SO_4 it was only the samples containing sand that agglomerated. In the table "severely agglomerated" particles were defined as the particles that were so fused to the crucible that they were not possible to retrieve the entire sample. "Agglomerated" particles were possible to recover but with some mechanical force.

All samples were analyzed with XRF to determine the elemental composition of the sample after furnace exposure. The results can be seen in Table 4. Important to notice is that all samples analyzed were in a reduced state. So even if only 4 % potassium was added, the amount of potassium detected using XRF may be higher due to the weight reduction of the reduced sample besides the decomposition of the carbonate, sulphate and phosphate ions. Here it can be concluded that the overall concentrations of potassium in the samples are similar to each other. Compared to previous studies, the potassium concentration was expected to be lower in LD slag samples compared to ilmenite and mixtures with sand. This since LD slag doth during operation in boiler [53] and in laboratory scale experiments [36] has indicated that LD slag does not bind as much potassium to in a stabile structure compared to ilmenite and sand. This could indicate that the evaporation rate of potassium is

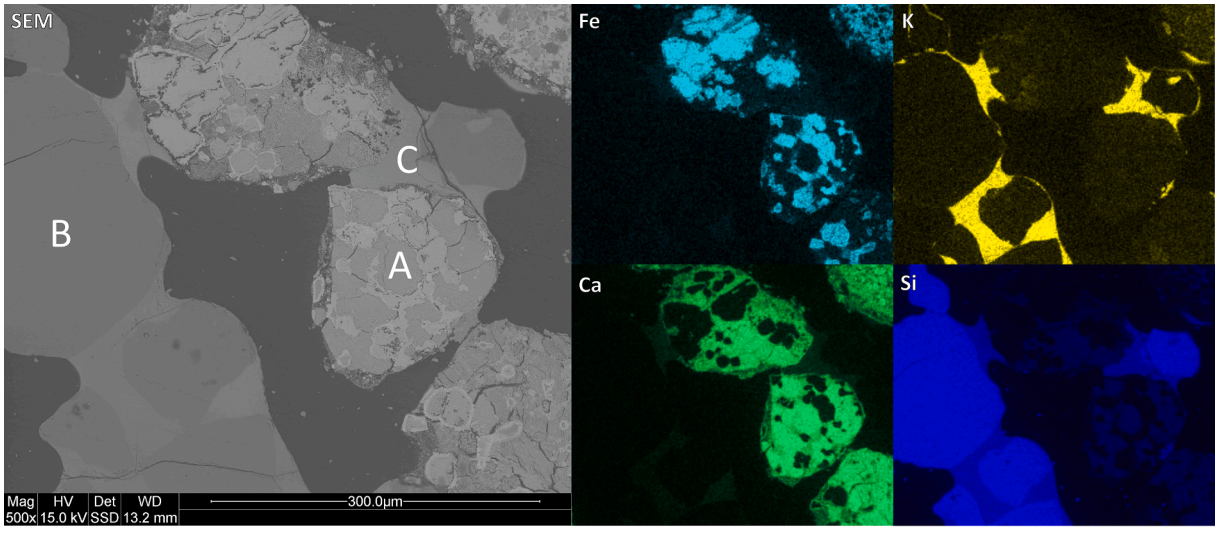

Fig. 5. Back-scattered SEM and elemental mapping micrographs of cross-sections of the reduced LD slag/sand (LDSA)-K_2CO_3 mix sample. A: LD slag particle, B: Sand particle, C: Melt of potassium silicate.

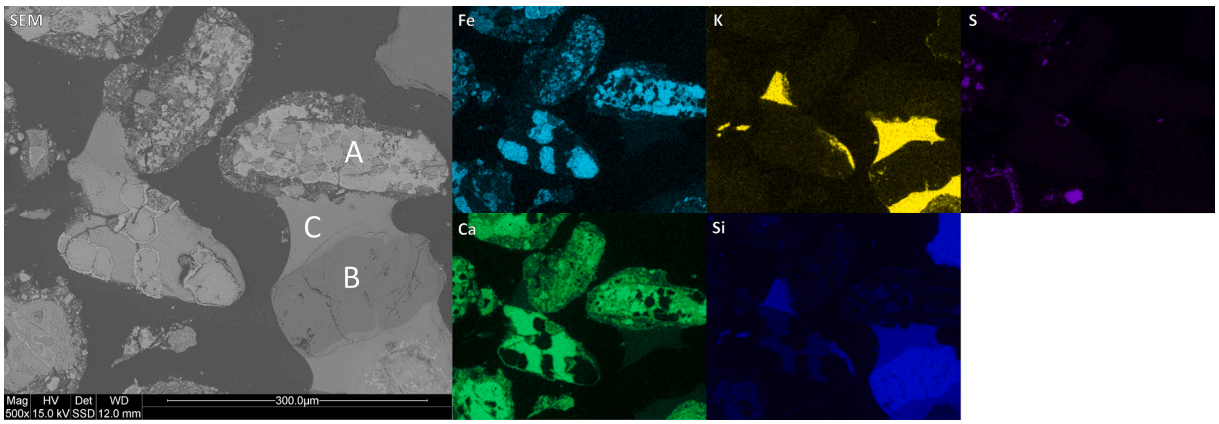

Fig. 6. Back-scattered SEM and elemental mapping micrographs of cross-sections of the reduced LD slag/sand (LDSA)-K_2SO_4 mix sample. A: LD slag particle, B: Sand particle, C: Melt of potassium silicate.

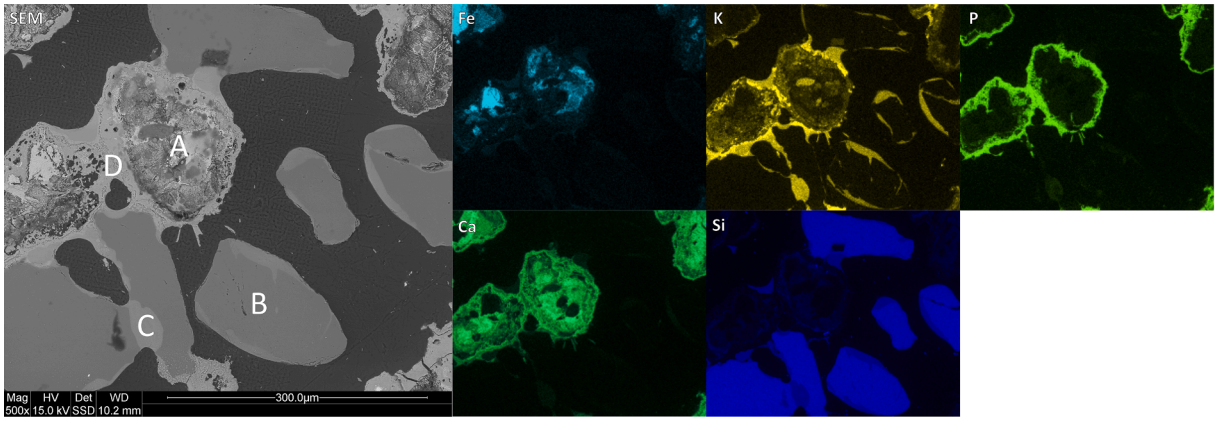

Fig. 7. Back-scattered SEM and elemental mapping micrographs of cross-sections of the reduced LD slag/sand (LDSA)-KH_2PO_4 mix sample. A: LD slag particle, B: Sand particle, C: Melt of potassium silicate, D: Ca-K-P phase.

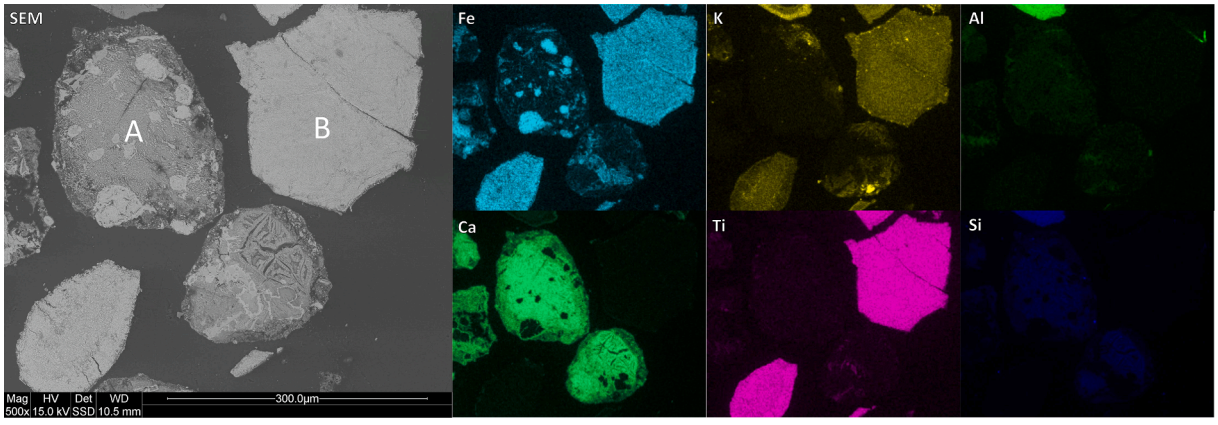

Fig. 8. Back-scattered SEM and elemental mapping micrographs of cross-sections of the reduced LD slag/ilmenite (ILLD)-K_2CO_3 mix sample. A: LD slag particle, B: ilmenite particle.

slow in this reaction setup where there is only a small flow of gases passing over the sample.

4. Conclusion

In this study, the material behavior of ilmenite, LD slag and their sand-diluted mixtures was investigated when exposed to three different potassium salts common in ash from biofuel. The exposures were executed in a fixed bed in a horizontal tubular furnace at 900 °C under reducing conditions with H_2 in presence of steam. The three potassium salts used in this study were K_2CO_3, K_2SO_4 and KH_2PO_4. From the experiments in this study, it was observed that potassium accumulated in ilmenite to a greater extent than in LD slag when LD slag and ilmenite were exposed together in the presence of either K_2CO_3 or K_2SO_4, no tendency of agglomeration could be observed. Then the mixture of oxygen carriers was exposed to KH_2PO_4, Ca from LD slag interacted with

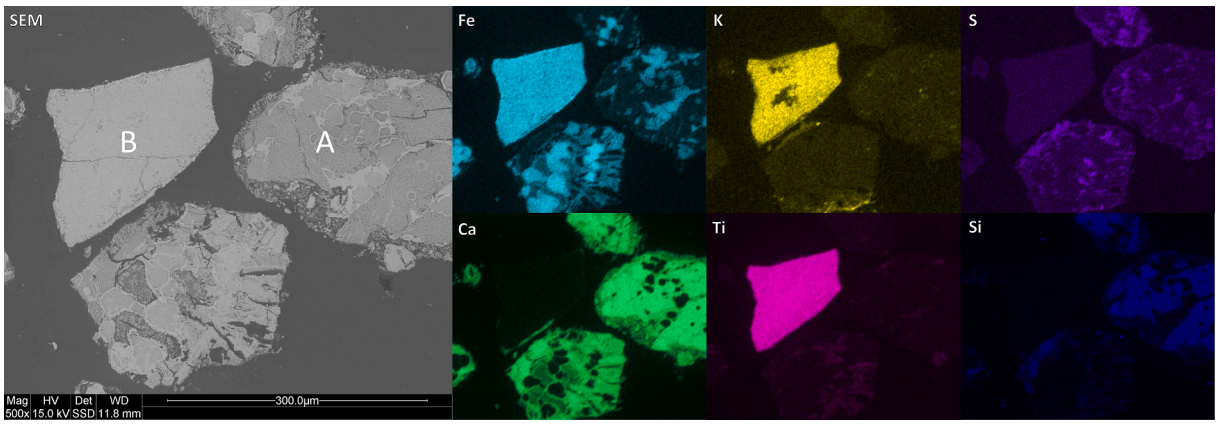

Fig. 9. Back-scattered SEM and elemental mapping micrographs of cross-sections of the reduced LD slag/ilmenite (ILLD)-K_2SO_4 mix sample. A: LD slag particle, B: ilmenite particle.

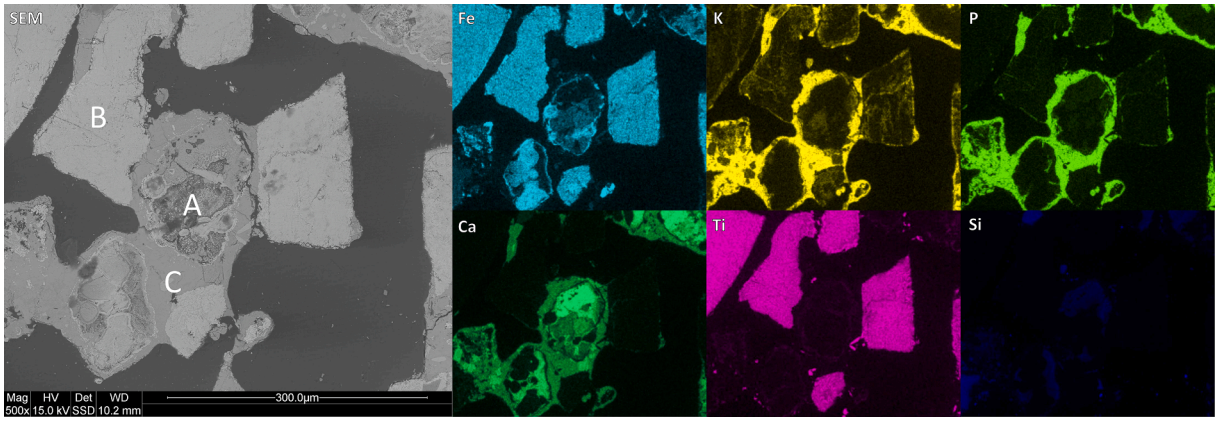

Fig. 10. Back-scattered SEM and elemental mapping micrographs of cross-sections of the reduced LD slag/ilmenite (ILLD)-KH_2PO_4 mix sample. A: LD slag particle, B: Sand particle, C: Melt of Ca-K-P phase.

Table 3
Agglomeration of samples exposed to reducing atmosphere in a horizontal furnace.

	No salt	K_2CO_3	K_2SO_4	KH_2PO_4
LD	None	None	None	Agglomerated
IL	None	None	None	Severely Agglomerated
ILLD	None	None	None	Agglomerated
LDSA	None	Severely Agglomerated	Agglomerated	Agglomerated
ILSA	None	Severely Agglomerated	Agglomerated	Agglomerated

the formed phosphate phase forming a K-Ca-P phase. This made the agglomeration less severe compared to when only ilmenite was exposed to KH_2PO_4 in the same conditions.

When silica sand was used to dilute either of the tested Fe-based oxygen carriers, a significant agglomeration was observed with all potassium salts. The agglomeration for both K_2CO_3 and K_2SO_4-containing samples was a result of the formation of potassium silicate with a low melting point. All samples with KH_2PO_4 agglomerated, but in different ways for the two oxygen carriers. When LD slag was diluted with silica sand, phosphorus was associated to a K-Ca-P phase while some potassium interacted with silica sand forming potassium silicates. With ilmenite, the agglomeration was a result of the formation of KPO_3, the same as without the presence of sand.

Table 4
Elemental composition given in wt-% detected with XRF of the samples after exposures in the tubular furnace. SUM indicates if the amount of oxides of the quantified elements add up to the sample weight.

	SUM	Si	P	K	Ca	Ti	Fe
LD-ref	84.7	4.5	0.2	0.0	29.0	0.7	15.2
LD-K_2CO_3	84.2	4.2	0.2	3.2	27.9	0.6	14.2
LD-K_2SO_4	86.5	3.8	0.2	4.4	26.5	0.6	13.7
LD-KH_2PO_4	87.8	3.6	3.8	4.1	25.9	0.6	13.5
IL-ref	88.8	1.6	0.0	0.0	0.3	22.6	29.6
IL-K_2CO_3	85.9	1.3	0.0	2.9	0.2	20.7	28.3
IL-K_2SO_4	91.4	1.2	0.0	5.3	0.2	20.7	26.4
IL-KH_2PO_4	90.6	2.6	4.7	4.6	13.4	10.5	18.5
ILLD-ref	91.8	3.5	0.2	0.1	16.4	12.5	22.0
ILLD-K_2CO_3	87.7	2.8	0.1	3.0	15.3	11.3	21.1
ILLD-K_2SO_4	89.3	2.7	0.1	4.3	14.5	11.0	19.4
ILLD-KH_2PO_4	90.6	2.6	4.7	4.6	13.4	10.5	18.5
ILSA-ref	88.4	21.8	0.0	0.3	0.1	11.3	13.9
ILSA-K_2CO_3	87.3	20.4	0.0	3.5	0.1	10.8	13.1
ILSA-K_2SO_4	90.1	18.5	0.0	4.5	0.1	11.4	13.7
ILSA-KH_2PO_4	81.5	14.3	4.5	4.7	0.1	9.3	11.6
LDSA-ref	77.6	18.4	0.2	0.3	14.7	0.4	7.3
LDSA-K_2CO_3	81.5	19.1	0.1	3.8	14.7	0.3	7.1
LDSA-K_2SO_4	84.7	18.6	0.1	4.1	15.0	0.3	7.3
LDSA-KH_2PO_4	84.9	15.4	4.5	4.5	14.4	0.3	6.8

To summarize, a mixture of LD slag and ilmenite could be beneficial for ash interaction due to the presence of additional lime. Sand for dilution should however be carefully evaluated if high alkali fuels are to

be used due to the risk of agglomeration with either oxygen carrier. However, as potassium containing species showed a tendency to interact with sand rather than the Fe-based oxygen carriers, the use of sand could also be used to prevent the alkali interaction of the oxygen carriers by the formation of potassium silicate.

CRediT authorship contribution statement

Fredrik Hildor: Writing – original draft, Writing – review & editing, Methodology, Data curation, Visualization, Supervision. **Duygu Yilmaz:** Writing – original draft, Methodology, Supervision. **Henrik Leion:** Supervision, Funding acquisition.

Declaration of Competing Interest

The authors declare that they have no known competing financial interests or personal relationships that could have appeared to influence the work reported in this paper.

Data availability

Data will be made available on request.

Acknowledgments

This work was funded by Chalmers Area of Advance Energy and ÅForsk (20-269). The LD slag bed material was provided by SSAB and the ilmenite by Titania A/S. The laboratory work was mainly done as a student project by Lina Håkansson, Patrick Jonsson, Hanna Karlsson Fernberg, Hanna Larsson, Harald Olivegren and Viktor Skans.

References

[1] Bui M, Adjiman CS, Bardow A, Anthony EJ, Boston A, Brown S, et al. Carbon Capture and Storage (CCS): The way forward. Energ Environ Sci 2018;11:1062–176. https://doi.org/10.1039/c7ee02342a.
[2] Olsson O, Bang C, Borchers M, Hahn A, Karjunen H, Thran D, et al. Deployment of BECCS / U value chains technological pathways. Policy Opt Business Models 2020.
[3] Haszeldine RS, Flude S, Johnson G, Scott V. Negative emissions technologies and carbon capture and storage to achieve the Paris Agreement Commitments. Philos Trans R Soc A Math Phys Eng Sci 2018;376. https://doi.org/10.1098/rsta.2016.0447.
[4] Pour N. Status of Bioenergy with Carbon Capture and Storage-Potential and Challenges. Bioenergy with Carbon Capture and Storage: Using Natural Resources for Sustainable Development 2019:85–107. https://doi.org/10.1016/B978-0-12-816229-3.00005-3.
[5] Lyngfelt A, Leckner B, Mattisson T. A Fluidized-Bed Combustion Process with Inherent CO2 Separation; Application of Chemical-Looping Combustion. Chem Eng Sci 2001;56:3101–13. https://doi.org/10.1016/S0009-2509(01)00007-0.
[6] Cho P, Mattisson T, Lyngfelt A. Comparison of Iron-, Nickel-, Copper- and Manganese-Based Oxygen Carriers for Chemical-Looping Combustion. Fuel 2004;83:1215–25. https://doi.org/10.1016/j.fuel.2003.11.013.
[7] Lyngfelt A. Chemical Looping Combustion. (CLC); 2013. ISBN 9780857095411.
[8] Wang P, Leion H, Yang H. Oxygen-Carrier-Aided Combustion in a Bench-Scale Fluidized Bed. Energy Fuel 2017;31:6463–71. https://doi.org/10.1021/acs.energyfuels.7b00197.
[9] Fredrik L, et al. 12,000 Hours of Operation with Oxygen-Carriers in Industrially Relevant Scale. VGB PowerTech 2017;7.
[10] Lyngfelt A. Chemical Looping Combustion: Status and Development Challenges. Energy Fuel 2020;34:9077–93. https://doi.org/10.1021/acs.energyfuels.0c01454.
[11] Jing D, Mattisson T, Leion H, Rydén M, Lyngfelt A. Examination of Perovskite Structure CaMnO3-δ with MgO Addition as Oxygen Carrier for Chemical Looping with Oxygen Uncoupling Using Methane and Syngas. Int J Chem Eng 2013;2013. https://doi.org/10.1155/2013/679560.
[12] Shulman A, Cleverstam E, Mattisson T, Lyngfel A. Manganese/Iron, Manganese/Nickel, and Manganese/Silicon Oxides Used in Chemical-Looping with Oxygen Uncoupling (CLOU) for Combustion of Methane. Energy Fuel 2009;23:5269–75. https://doi.org/10.1021/ef9005466.
[13] Mattisson T, Järdnäs A, Lyngfelt A. Reactivity of Some Metal Oxides Supported on Alumina with Alternating Methane and Oxygen - Application for Chemical-Looping Combustion. Energy Fuel 2003;17:643–51. https://doi.org/10.1021/ef020151i.
[14] Adánez-Rubio I, Pérez-Astray A, Abad A, Gayán P, De Diego LF, Adánez J. Chemical Looping with Oxygen Uncoupling: An Advanced Biomass Combustion Technology to Avoid CO2 Emissions. Mitig Adapt Strat Glob Chang 2019;24:1293–306. https://doi.org/10.1007/s11027-019-9840-5.
[15] Khan AA, de Jong W, Jansens PJ, Spliethoff H. Biomass Combustion in Fluidized Bed Boilers: Potential Problems and Remedies. Fuel Process Technol 2009;90:21–50. https://doi.org/10.1016/j.fuproc.2008.07.012.
[16] Zevenhoven M, Yrjas P, Skrifvars BJ, Hupa M. Characterization of Ash-Forming Matter in Various Solid Fuels by Selective Leaching and Its Implications for Fluidized-Bed Combustion. Energy Fuel 2012;26:6366–86. https://doi.org/10.1021/ef300621j.
[17] Rydén M, Leion H, Mattisson T, Lyngfelt A. Combined Oxides as Oxygen-Carrier Material for Chemical-Looping with Oxygen Uncoupling. Appl Energy 2014;113:1924–32. https://doi.org/10.1016/J.APENERGY.2013.06.016.
[18] Adánez J, De Diego LF, García-Labiano F, Gayán P, Abad A, Palacios JM. Selection of Oxygen Carriers for Chemical-Looping Combustion. Energy Fuel 2004;18:371–7. https://doi.org/10.1021/ef0301452.
[19] Imtiaz Q, Hosseini D, Müller CR. Review of Oxygen Carriers for Chemical Looping with Oxygen Uncoupling (CLOU): Thermodynamics, Material Development, and Synthesis. Energ Technol 2013;1:633–47.
[20] Störner F, Lind F, Rydén M. Oxygen Carrier Aided Combustion in Fluidized Bed Boilers in Sweden—Review and Future Outlook with Respect to Affordable Bed Materials. Appl Sci (Switzerland) 2021;11:7935. https://doi.org/10.3390/app11177935.
[21] Corcoran A, Marinkovic J, Lind F, Thunman H, Knutsson P, Seemann M. Ash Properties of Ilmenite Used as Bed Material for Combustion of Biomass in a Circulating Fluidized Bed Boiler. Energy Fuel 2014;28:7672–9. https://doi.org/10.1021/ef501810u.
[22] Hildor F, Leion H, Linderholm CJ, Mattisson T. Steel Converter Slag as an Oxygen Carrier for Chemical-Looping Gasification. Fuel Process Technol 2020;210:106576. https://doi.org/10.1016/j.fuproc.2020.106576.
[23] Tossavainen M, Engstrom F, Yang Q, Menad N, Lidstrom Larsson M, Bjorkman B. Characteristics of Steel Slag under Different Cooling Conditions. Waste Manag 2007;27:1335–44. https://doi.org/10.1016/j.wasman.2006.08.002.
[24] Condori O, García-Labiano F, de Diego LF, Izquierdo MT, Abad A, Adánez J. Biomass Chemical Looping Gasification for Syngas Production Using LD Slag as Oxygen Carrier in a 1.5 KWth Unit. Fuel Process Technol 2021;222. https://doi.org/10.1016/j.fuproc.2021.106963.
[25] Yilmaz D, Leion H. Interaction of Iron Oxygen Carriers and Alkaline Salts Present in Biomass-Derived Ash. Energy Fuel 2020;34:11143–53. https://doi.org/10.1021/acs.energyfuels.0c02109.
[26] Niu Y, Tan H, Hui S. Ash-Related Issues during Biomass Combustion: Alkali-Induced Slagging, Silicate Melt-Induced Slagging (Ash Fusion), Agglomeration, Corrosion, Ash Utilization, and Related Countermeasures. Prog Energy Combust Sci 2016;52:1–61. https://doi.org/10.1016/j.pecs.2015.09.003.
[27] Miles TR, Baxter LL, Bryers RW, Jenkins BM, Oden LL. Alkali Deposits Found in Biomass Power Plants, Vol 1. NREL report 1995;I:1–122.
[28] Zhao X, Zhou H, Sikarwar VS, Zhao M, Park AHA, Fennell PS, et al. Biomass-Based Chemical Looping Technologies: The Good, the Bad and the Future. Energ Environ Sci 2017;10:1885–910. https://doi.org/10.1039/c6ee03718f.
[29] Zevenhoven, M.; Yrjas, P.; Hupa, M. 14 Ash-Forming Matter and Ash-Related Problems. In *Handbook of Combustion Vol.4: Solid Fuels*; Lackner, M., Winter, F., Agarwal, A.K., Eds.; WILEY-VCH Verlag GmbH & Co. KGaA, 2010; pp. 493–531 ISBN 978-3-527-32449-1.
[30] Miao Z, Jiang E, Hu Z. Review of Agglomeration in Biomass Chemical Looping Technology. Fuel 2022;309:122199. https://doi.org/10.1016/j.fuel.2021.122199.
[31] Gatternig B, Karl J. Investigations on the Mechanisms of Ash-Induced Agglomeration in Fluidized-Bed Combustion of Biomass. Energy Fuel 2015;29:931–41. https://doi.org/10.1021/ef502658b.
[32] Elled AL, Åmand LE, Steenari BM. Composition of Agglomerates in Fluidized Bed Reactors for Thermochemical Conversion of Biomass and Waste Fuels: Experimental Data in Comparison with Predictions by a Thermodynamic Equilibrium Model. Fuel 2013;111:696–708. https://doi.org/10.1016/j.fuel.2013.03.018.
[33] Yilmaz D, Steenari BM, Leion H. Comparative Study: Impacts of Ca and Mg Salts on Iron Oxygen Carriers in Chemical Looping Combustion of Biomass. ACS Omega 2021. https://doi.org/10.1021/acsomega.1c02138.
[34] Darwish E, Yllmaz D, Leion H. Experimental and Thermodynamic Study on the Interaction of Copper Oxygen Carriers and Oxide Compounds Commonly Present in Ashes. Energy Fuel 2019;33:2502–15. https://doi.org/10.1021/acs.energyfuels.8b04060.
[35] Gu H, Shen L, Zhong Z, Zhou Y, Liu W, Niu X, et al. Interaction between Biomass Ash and Iron Ore Oxygen Carrier during Chemical Looping Combustion. Chem Eng J 2015;277:70–8. https://doi.org/10.1016/j.cej.2015.04.105.
[36] Störner F, Hildor F, Leion H, Zevenhoven M, Hupa L, Rydén M. Potassium Ash Interactions with Oxygen Carriers Steel Converter Slag and Iron Mill Scale in Chemical-Looping Combustion of Biomass-Experimental Evaluation Using Model Compounds. Energy Fuel 2020;34:2304–14. https://doi.org/10.1021/acs.energyfuels.9b03616.
[37] Hildor F, Zevenhoven M, Brink A, Hupa L, Leion H. Understanding the Interaction of Potassium Salts with an Ilmenite Oxygen Carrier under Dry and Wet Conditions. ACS Omega 2020;5:22966–77. https://doi.org/10.1021/acsomega.0c02538.
[38] Hildor F, Mattisson T, Leion H, Linderholm C, Rydén M. Steel Converter Slag as an Oxygen Carrier in a 12 MWth CFB Boiler – Ash Interaction and Material Evolution. Int J Greenhouse Gas Control 2019;88:321–31. https://doi.org/10.1016/j.ijggc.2019.06.019.
[39] Corcoran A, Knutsson P, Lind F, Thunman H. Mechanism for Migration and Layer Growth of Biomass Ash on Ilmenite Used for Oxygen Carrier Aided Combustion. Energy Fuel 2018;32:8845–56. https://doi.org/10.1021/acs.energyfuels.8b01888.

[40] Rydén M, Hanning M, Corcoran A, Lind F. Oxygen Carrier Aided Combustion (OCAC) of Wood Chips in a Semi-Commercial Circulating Fluidized Bed Boiler Using Manganese Ore as Bed Material. Appl Sci (Switzerland) 2016;6:1–19. https://doi.org/10.3390/app6110347.
[41] Rydén M, Hanning M, Lind F. Oxygen Carrier Aided Combustion (OCAC) of Wood Chips in a 12 MWth Circulating Fluidized Bed Boiler Using Steel Converter Slag as Bed Material. Appl Sci 2018;8:2657. https://doi.org/10.3390/app8122657.
[42] Dieringer P, Marx F, Alobaid F, Ströhle J, Epple B. Process Control Strategies in Chemical Looping Gasification-A Novel Process for the Production of Biofuels Allowing for Net Negative CO2 Emissions. Appl Sci (Switzerland) 2020;10:4271. https://doi.org/10.3390/app10124271.
[43] Teyssié G, Leion H, Schwebel GL, Lyngfelt A, Mattisson T. Influence of Lime Addition to Ilmenite in Chemical-Looping Combustion (CLC) with Solid Fuels. Energy Fuel 2011;25:3843–53. https://doi.org/10.1021/ef200623h.
[44] Miles TR, Baxter LL, Bryers RW, Jenkins BM, Oden LLA. Deposits Found in Biomass Power Plants 1996;II.
[45] Staničić I, Brorsson J, Hellman A, Mattisson T, Backman R. Thermodynamic Analysis on the Fate of Ash Elements in Chemical Looping Combustion of Solid Fuels Iron-Based Oxygen Carriers. Energy Fuel 2022. https://doi.org/10.1021/acs.energyfuels.2c01578.
[46] Zevenhoven M, Sevonius C, Salminen P, Lindberg D, Brink A, Yrjas P, et al. Defluidization of the Oxygen Carrier Ilmenite – Laboratory Experiments with Potassium Salts. Energy 2018;148:930–40. https://doi.org/10.1016/j.energy.2018.01.184.
[47] Brown ME, Glasser L, Larson J. High Temperature Thermal Properties of KH2PO4: Phase Transitions and Decompositions. Thermochim Acta 1979;30:233–46. https://doi.org/10.1016/0040-6031(79)85057-1.
[48] Wu H, Castro M, Jensen PA, Frandsen FJ, Glarborg P, Dam-Johansen K, et al. Release and Transformation of Inorganic Elements in Combustion of a High-Phosphorus Fuel. Energy Fuel 2011;25:2874–86. https://doi.org/10.1021/EF200454Y/SUPPL_FILE/EF200454Y_SI_001.PDF.
[49] Bao J, Li Z, Cai N. Interaction between Iron-Based Oxygen Carrier and Four Coal Ashes during Chemical Looping Combustion. Appl Energy 2014;115:549–58. https://doi.org/10.1016/j.apenergy.2013.10.051.
[50] Chand S, Paul B, Kumar M. Sustainable Approaches for LD Slag Waste Management in Steel Industries: A Review. Metallurgist 2016;60:116–28. https://doi.org/10.1007/s11015-016-0261-3.
[51] Barišić V, Åmand LE, Coda Zabetta E. The Role of Limestone in Preventing Agglomeration and Slagging during CFB Combustion of High Phosphorus Fuels. In: Proceedings of the World Bioenergy. Swedish Bioenergy Association; 2008. p. 1–6.
[52] Lindström E, Sandström M, Boström D, Öhman M. Slagging Characteristics during Combustion of Cereal Grains Rich in Phosphorus. Energy Fuel 2007;21:710–7. https://doi.org/10.1021/ef060429x.
[53] Hildor F, Mattisson T, Leion H, Linderholm C, Rydén M. Steel Converter Slag as an Oxygen Carrier in a 12 MW_{th} CFB Boiler – Ash Interaction and Material Evolution. Int J Greenhouse Gas Control 2019;88. https://doi.org/10.1016/j.ijggc.2019.06.019.